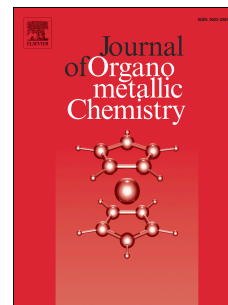# Accepted Manuscript

B-phenylated o-carboranes and its chromium derivatives: Synthesis, electrochemical properties, and X-ray structural studies

So-Yoen Kim, So-Young Ma, Sang Ook Kang, Jong-Dae Lee

B-Phenylated o-carboranes and its chromium derivatives: Synthesis, electrochemical properties, and X-ray structural studies

So-Yoen Kim,[†] So-Young Ma,[†] Sang Ook Kang,[†] Jong-Dae Lee[‡,*]

†Department of Advanced Materials Chemistry, College of Science and Technology, Korea University, 2511 Sejong-ro, Sejong 30019, South Korea

‡Department of Chemistry, College of Natural Sciences, Chosun University, 309 Pilmundaero, Gwangju 61452, South Korea

Abstract

The electron accepting capability of B-phenylated o-carborane is greatly improved through favorable electronic interactions between the two adjoining phenyl-π^* and cage carbon-σ^* orbitals. Phenyl substitution at the boron atom in the 3-position directs the two phenyl groups of the cage carbon atoms to a face-to-face position and locks them into a rigid conformation, which gives rise to extensive electronic delocalization and maximum energy stabilization from the lowest unoccupied molecular orbital (LUMO). A reversible reduction peak from the cyclovoltammogram (CV) at −1.72 V and a broad and extended UV absorption (λ_{max} = 277 nm) substantiate such LUMO stabilization, thereby augmenting the electron accepting capability of o-carborane. Due to electron depletion from the adjacent o-carborane, the adjoined phenyl groups act as potential π-acid; indeed, when B-phenylated 1,2-diphenyl-o-carborane was reacted with $Cr(CO)_6$, bi- and trimetallic chromium complexes were selectively formed in an η^6-bonding fashion between the chromium atoms and phenyl groups.

1. Introduction

It has been suggested that o-carborane acts as an effective electron acceptor [1], and its application toward electronic structure modification has been the subject of much interest in both organic [2] and organometallic [3] chemistry. However, other than a few reports on the electron withdrawing characteristics of o-carborane as an organic functional group, a detailed study that elaborates on its origin is absent [4]. Recently, it was found that the σ^* orbital of o-carborane is mainly derived from the cage carbon atoms and is greatly stabilized by the addition of adjacent phenyl groups on the same carbon atoms [5]. Orbital analysis revealed that the LUMO constitutes o-carboranyl C−C σ^* and adjacent phenyl π^* orbitals. Since the o-carboranyl C−C σ^* orbital is directly bonded to the aromatic groups, through a π^* orbital, the electron-accepting capability of o-carborane seems closely related to the LUMO participation of the phenyl groups at the cage carbon atoms.

The C1−C2 bond in o-carborane is well known for its elasticity [6,7]. Unsubstituted o-carborane itself has a

C–C bond length of 1.62 Å [8], which can be elongated up to 2.15 Å [9] with bulky substituents at both C1 and C2 and up to 2.42 Å [10] by substituents capable of forming multiple bonds with one of the carborane C atoms. Recently, molecules containing the 1,2-diphenyl-o-carborane unit were reported to have remarkable luminescence properties, with the excited electron being transferred from the aromatic ring to the cluster after excitation [11]. It is assumed that the excited-state geometries in diaryl-o-carboranes contain long C1–C2 distances as in their corresponding radical anions [5,12,13]. In order to examine whether the bond elongation in 1,2-diphenyl-*o*-carborane results from either steric [14] or electronic effects, we have chosen B-phenylated 1,2-diphenyl-*o*-carborane and its chromium complexes as model compounds. Transition-metal π complexes are widely used in organic and organometallic chemistry for various catalytic and synthetic tasks. In particular, the η^6-arene complexes of chromium have been the subject of extensive development due to their significant applications in organic synthesis [15]. Moreover, the use of metal carbonyls in bioorganometallic chemistry is increasingly being developed, enhancing the potential of Cr complexes in this field [16,17].

In this study, systematic phenyl group substitution was carried out at the carbon, boron, or both atoms adjacent to each other (i.e., positions 1, 2, 3, and 6 of the cage carborane) to characterize the corresponding changes on the arene–carborane dihedral angles in B-phenylated triphenyl-o-carborane and its chromium complexes by X-ray structural studies.

2. Experimental section

2.1 Materials and instruments

All manipulations were performed in a dry nitrogen or argon atmosphere using standard Schlenk techniques. Tetrahydrofuran (THF) was distilled under nitrogen from sodium/benzophenone. The elemental analyses were performed using a Carlo Erba Instruments CHNS-O EA 1108 analyzer. High Resolution Tandem Mass Spectrometry (Jeol LTD JMS-HX 110/110A) was performed at the Korean Basic Science Institute. The ^{1}H, ^{11}B, and ^{13}C NMR spectra were recorded on a Bruker 600 spectrometer operating at 600.1, 150.9, and 192.6 MHz, respectively. All ^{11}B chemical shifts were referenced to $BF_3 \cdot O(C_2H_5)_2$ (0.0 ppm) with a negative sign indicating an up-field shift. All proton and carbon chemical shifts were measured relative to the internal residual $CHCl_3$ from the lock solvent (99.9% $CDCl_3$). The absorption and photoluminescence spectra were recorded on a SHIMADZU UV-3101PC UV-VIS-NIR scanning spectrophotometer and a VARIAN Cary Eclipse fluorescence spectrophotometer, respectively. Decaborane, o-carborane, and 1-phenyl-o-carborane were purchased from Katchem and *N,N*-dimethylaniline, 1,2-diphenylacetylene, dichlorophenylborane, n-BuLi (2.5 M in hexane), chromium hexacarbonyl [$Cr(CO)_6$], and benzene-chromium(0) tricarbonyl [$(\eta^6\text{-Bz})Cr(CO)_3$] were purchased from Aldrich Chemicals.

2.2 Crystal structure determination

Crystals of **1**, **2**, **3**, **4**, and **5** were obtained from toluene or CH_2Cl_2, sealed in glass capillaries under argon, and mounted on the diffractometer. Preliminary examination and data collection were performed using a Bruker

SMART CCD detector system single-crystal X-ray diffractometer equipped with a sealed-tube X-ray source (40 kV × 50 mA) using graphite-monochromated Mo Kα radiation (λ = 0.71073 Å). Preliminary unit cell constants were determined with a set of 45 narrow-frame (0.3° in ω) scans. The double-pass method of scanning was used to exclude any noise. The collected frames were integrated using an orientation matrix determined from the narrow-frame scans. The SMART software package was used for data collection, and SAINT was used for frame integration [18]. Final cell constants were determined by a global refinement of *xyz* centroids of reflections harvested from the entire data set. Structure solution and refinement were carried out using the SHELXTL-PLUS software package [19].

2.3 Cyclic voltammetry

The cyclic voltammetry experiments were performed using a BAS 100 electrochemical analyzer. A three-electrode cell system containing a platinum disk, a platinum wire, and $Ag/AgNO_3$ as the working, counter, and reference electrodes, respectively, was used. All data were obtained for Ar-purged CH_2Cl_2 solution containing 0.1M tetrabutylammonium perchlorate (TBAP) at a scan rate of 0.1 V s^{-1}.

2.4 Raman spectroscopy

Raman spectra were obtained using a micro-Raman system (JY-Horiba, LabRam 300) with a collimated 50 x objective lens (Olympus, NA 0.75). This system is equipped with a thermoelectrically cooled charged-coupled device (CCD) detector and the signal was obtained by 180° backscattering geometry. The 647 nm line of CW Kr ion laser (Coherent, Innova 300C) was used as a Raman excitation source.

2.5 Density functional calculations

Full geometry optimizations of the complexes in their singlet ground state were performed with DFT using the B3LYP functional [20], with the relativistic effective core potential and basis set LanL2DZ [21] for the chromium and the 6-31G(d) [22] basis set for the remaining atoms. No symmetry constraints were applied during the geometry optimizations, which were carried out with the Gaussian 09 package [23]. The nature of the stationary points located was further checked by computations of harmonic vibrational frequencies at the same level of theory. All isodensity plots (isodensity contour = 0.03 a.u.) of the frontier orbitals were visualized by Chem3D Ultra [24]. The highest occupied molecular orbitals (HOMOs), LUMOs, and their energy gaps of all compounds were obtained from the computed results and were compared with the available experimental data. The excitation energies and the oscillator strengths for the 30 lowest singlet–singlet transitions at the optimized ground-state geometries were obtained with TDDFT calculations using the identical level of theory as that used for the ground state. Likewise, frequency calculations of all geometry-optimized carboranes, including Raman data, were calculated using the same level of theory. Simulated absorption spectra and Raman spectra of all carborane compounds were obtained by GaussSum 2.2 [25].

2.6 Synthesis of 1,2,3-triphenyl-o-carborane (*1*)

1,2-Diphenyl-o-carborane (1.10 g, 5.0 mmol) was added to a solution of KOH (0.84 g, 15 mmol) in 50 mL of ethanol and the clear reaction mixture was heated to reflux. TLC of the reaction mixture sample showed no

starting material spot after that time. The reaction mixture was evaporated to dryness and re-dissolved in 50 mL of distilled water. An excess of Me_4NCl was added to the reaction mixture and the precipitate of the tetramethylammonium nido-carborane salt formed was filtered off and dried using air suction (1.42 g, 100%). A 2.5 M solution of n-BuLi in hexane (1.0 mL, 2.2 mmol) was slowly added dropwise to a stirred solution of tetramethylammonium nido-carborane salt (0.57 g, 2.0 mmol) in 40 mL of THF at −78 °C, and then dichlorophenylborane (0.35 g, 2.2 mmol) was added *via* cannula. The reaction mixture was then left to warm to room temperature and then heated to reflux for 6 h. The white precipitate of lithium chloride was removed by filtration in air and washed with THF. After evaporation, the crude reaction mixture was purified by column chromatography (with hexane as the eluent) to give 1,2,3-triphenyl-o-carborane **1**, which was then recrystallized from toluene to obtain white crystals. Yield: 86% (0.64 g, 1.72 mmol). m.p.: 193−194 °C. HRMS: Calcd for $[^{12}C_{20}{}^{11}B_{10}{}^{1}H_{24}]^+$ 374.2809. Found: 374.2802. IR spectrum (KBr pellet, cm^{-1}): ν(B−H) 2581, 2601; ν(C−H) 3237. ^1H NMR (CDCl$_3$, 600.1 MHz) δ 7.410 (m, 4H, Ph-*H*), 7.310 (m, 3H, Ph-*H*), 7.150 (m, 8H, Ph-*H*). ^{13}C NMR (CDCl$_3$, 150.9 MHz) δ 135.6, 131.3, 131.0, 129.9, 128.9, 128.0, 127.36 (*Ph*), 83.6 (Ph-*C*cab). ^{11}B NMR (CDCl$_3$, 192.6 MHz) δ −1.62 (1B), −2.99 (2B), −8.02 (3B), −8.57 (2B), −10.15 (2B).

2.7 Synthesis of 1,3,6-triphenyl-o-carborane (2)

A procedure analogous to the preparation of **1** was used and obtained white crystals. Yield: 58% (0.43 g, 1.2 mmol). m.p.: 178−179 °C. HRMS: Calcd for $[^{12}C_{20}{}^{11}B_{10}{}^{1}H_{24}]^+$ 374.2809. Found: 374.2819. IR spectrum (KBr pellet, cm^{-1}): ν(B−H) 2581, 2601; ν(C−H) 3237. ^1H NMR (CDCl$_3$, 600.1 MHz) δ 7.334 (d, 4H, *J* = 7.8 Hz), 7.218 (d, 1H, *J* = 7.2 Hz), 7.206 (d, 1H, *J* = 7.8 Hz), 7.129 (d, 2H, *J* = 7.2 Hz), 7.117 (d, 2H, *J* = 7.8 Hz), 7.001 (t, 1H, *J* = 7.2 Hz), 6.900 (d, 1H, *J* = 8.4 Hz), 6.887 (d, 1H, *J* = 7.2 Hz), 6.791 (d, 2H, *J* = 7.8 Hz), 4.433 (s, 1H). ^{13}C NMR (CDCl$_3$, 150.9 MHz) δ 133.7, 130.5, 129.2, 128.6, 127.7, 127.6, 127.1 (*Ph*), 78.3 (Ph-*C*cab), 57.8 (H-*C*cab). ^{11}B NMR (CDCl$_3$, 192.6 MHz) δ −0.88 (2B), −2.77 (1B), −4.82 (1B), −9.75 (2B), −11.04 (2B), −14.05 (2B).

2.8 Synthesis of 1,2,3,6-tetraphenyl-o-carborane (3)

A procedure analogous to the preparation of **1** was used and obtained white crystals. Yield: 37% (0.33 g, 0.74 mmol). m.p.: 252-253 °C. HRMS: Calcd for $[^{12}C_{26}{}^{11}B_{10}{}^{1}H_{28}]^+$ 450.3122. Found: 450.3108. IR spectrum (KBr pellet, cm^{-1}): ν(B−H) 2581, 2601; ν(C−H) 3237. ^1H NMR (CDCl$_3$, 600.1 MHz) δ 7.294 (d, 4H, *J* = 7.8 Hz, Ph-*H*), 7.242 (d, 4H, *J* = 8.4 Hz, Ph-*H*), 7.229 (d, 4H, *J* = 7.8 Hz, Ph-*H*), 7.138 (d, 2H, *J* = 7.2 Hz, Ph-*H*), 7.126 (d, 2H, *J* = 7.8 Hz, Ph-*H*), 6.991 (t, 4H, *J* = 7.8 Hz, Ph-*H*). ^{13}C NMR (CDCl$_3$, 150.9 MHz) δ 134.6, 132.0, 130.2, 129.5, 128.9, 127.6, 127.1 (*Ph*), 80.3 (Ph-*C*cab). ^{11}B NMR (CDCl$_3$, 192.6 MHz) δ 1.44 (2B), −2.75 (2B), −8.50 (2B), −9.45 (4B).

2.9 Synthesis of 1,2-bis(phenyl-η^6-chromium(0)tricarbonyl)-3-phenyl-o-carborane (4)

Compound **1** (0.37 g, 1.0 mmol) and [Cr(CO)$_6$] (0.44 g, 2.0 mmol) were dissolved in a mixture of THF (5 mL) and di-*n*-butyl ether (50 mL). The mixture was refluxed for 72 h and the resulting dark reddish solution was cooled to room temperature and filtered over Celite. The solvents were evaporated under reduced pressure. After evaporation the crude reaction mixture was purified using column chromatography [CH$_2$Cl$_2$:Hexane (1:1) eluent]

to give chromium complex **4**, which was then recrystallized from toluene to obtain red crystals. Yield: 87% (0.59 g, 0.87 mmol). HRMS: Calcd for $[^{12}C_{26}{}^{1}H_{24}{}^{11}B_{10}{}^{52}Cr_2{}^{16}O_6]^+$ 646.1314. Found: 646.1322. IR spectrum (KBr pellet, cm^{-1}): ν(B$-$H) 2583, 2589; ν(CO) 1960, 1892. ^{1}H NMR (CDCl$_3$, 300.1 MHz) δ 7.62 (m, 4H, Ph-*H*), 7.47 (m, 3H, Ph-*H*), 7.30 (m, 8H, Ph-*H*). ^{13}C NMR (CDCl$_3$, 75.4 MHz) δ 231.4 (Cr-*C*O), 141.5, 137.9, 134.8, 132.7, 131.3, 130.8, 128.7 (*Ph*), 85.6 (Ph-*C*cab). ^{11}B NMR (CDCl$_3$, 96.3 MHz) δ −1.84 (1B), −3.11 (3B), −8.54 (3B), −8.71 (2B), −10.37 (1B).

*2.10 Synthesis of 1,2,3-tris(phenyl-η^6-chromium(0)tricarbonyl)-o-carborane (**5**)*

A procedure analogous to the preparation of **4** was used and obtained red crystals. Yield: 31% (0.24 g, 0.31 mmol). HRMS: Calcd for $[^{12}C_{29}{}^{1}H_{24}{}^{11}B_{10}{}^{52}Cr_3{}^{16}O_9]^+$ 782.0566. Found: 782.0594. IR spectrum (KBr pellet, cm^{-1}): ν(B$-$H) 2583, 2589; ν(CO) 1960, 1890. ^{1}H NMR (CDCl$_3$, 300.1 MHz) δ 7.70 (m, 4H, Ph-*H*), 7.48 (m, 3H, Ph-*H*), 7.33 (m, 8H, Ph-*H*). ^{13}C NMR (CDCl$_3$, 75.4 MHz) δ 233.1 (Cr-*C*O), 141.5, 140.3, 138.5, 135.1, 133.8, 131.1 (*Ph*), 85.6 (Ph-*C*cab). ^{11}B NMR (CDCl$_3$, 96.3 MHz) δ −1.87 (1B), −3.15 (2B), −8.60 (3B), −8.73 (2B), −10.40 (2B).

3. Results and Discussion

3.1 Synthesis of B-phenylated o-carboranes and its chromium derivatives

Starting from mono-phenylated or di-phenylated o-carborane [26], 1-phenyl- (PhC) or 1,2-diphenyl-o-carborane (Ph2C2), tri-phenylated 1,2,3-Ph$_3$-C$_2$B (**1**) and 1,2,6-Ph$_3$-CB$_2$ (**2**) and tetra-phenylated 1,2,3,6-Ph$_4$-C$_2$B$_2$ (**3**) o-carboranes were prepared in moderate yields (37 ~ 86%) [27]. As shown in Scheme 1, we first carried out phenyl substitutions on either/both 1,2-carbons and/or 3,6-borons of the icosahedral o-carborane framework. Depending on the substitution site at either the boron or carbon atom, their ^{11}B NMR spectra showed either symmetrical or asymmetrical patterns [28]; the most asymmetrical pattern was obtained for Ph2CB, followed by **1** and **2**, which are related by the extent of boron substitution. The most symmetrical pattern was obtained for the tertra-phenylated compound (**3**).
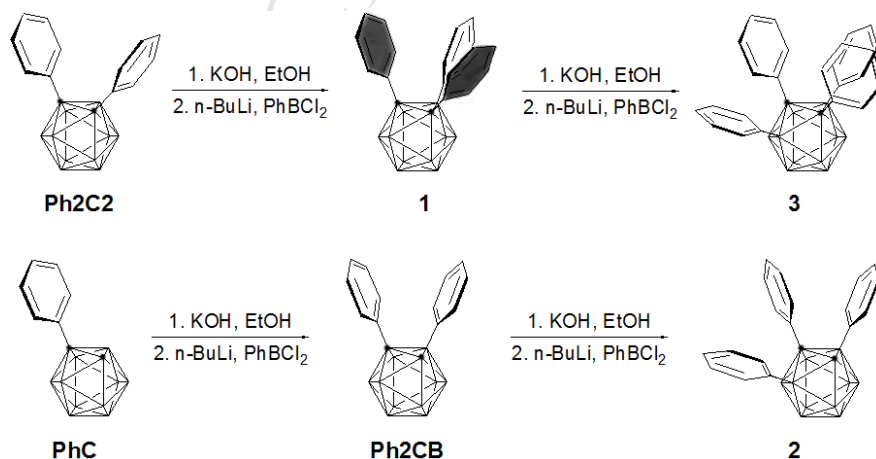
Scheme 1. Preparation of B-phenylated o-carborane derivatives (**1**, **2**, and **3**)

To establish the electron withdrawing capability of o-carborane, an organometallic π-donor functional group has been introduced to the phenyl groups [29]; the reaction of **1** with $Cr(CO)_6$ produced phenyl-coordinated bis- and tris-chromium complexes (**4** and **5**) in moderate yields, as shown in Scheme 2.
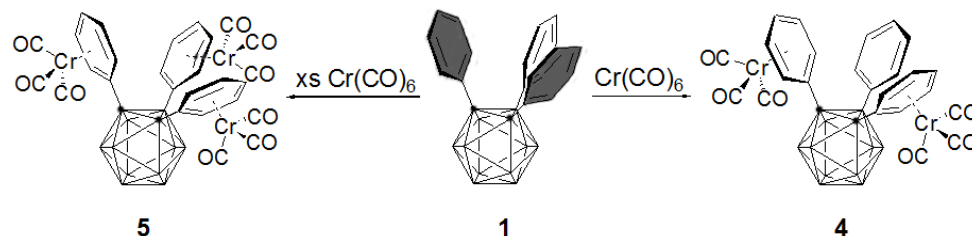
Scheme 2. Preparation of bis- and tris-chromium complexes (**4** and **5**).

3.2 IR and NMR spectroscopy

The structures of B-phenylated o-carboranes **1**, **2**, and **3** were proposed based on the assignment of their corresponding ^1H, ^{11}B, and ^{13}C NMR resonances. The ^1H NMR spectrum showed resonances at around δ 7.125 ~ 7.416 (**1**), 6.784 ~ 7.340 (**2**), and 6.978 ~ 7.300 (**3**) for the phenyl rings, respectively, and δ 4.433 for the carborane C–H (**2**). The ^{11}B NMR spectrum showed resonances at around δ −10.58 ~ −1.70 (**1**), −14.42 ~ −0.88 (**2**), and −9.81 ~ 1.40 (**3**), respectively. The ^{13}C NMR spectrum showed very similar resonances at around δ 127 ~ 135 for the B-phenylated o-carboranes. Compounds **4** and **5** exhibits characteristic absorption bands in the infrared spectra at 1960, 1892 (**4**) and 1960, 1890 cm^{-1} (**5**), reflecting the C≡O units. These values are shorter than that of $(C_6H_6)Cr(CO)_3$ [30]. The NMR spectra clearly show the Cr coordination of the phenyl groups of **4** and **5**, with the chemical shifts of δ 7.30 ~ 7.72 and 128.7 ~ 143.5 in the ^1H and ^{13}C NMR spectra, respectively.

3.3 Photophysical and electrochemical properties

Based on the UV spectral comparison between **1** and Ph2C2 shown in Figure 1, the absorptions arise mainly from phenyl units at the carbon atom, even though they are at low intensities. Given that the single carbon substitution in PhC exhibits a bathochromic shift due to the electron withdrawing character of o-carborane [31], further boron substitution does not exert much effect on the electronic structure, as evidenced by the UV spectrum of **2**. It is found that the new excited state is greatly influenced by the phenyl groups at the carbon atom, and the resultant electronically viable vibronic modes are reminiscent of the direct interaction between the σ* orbital of the C–C bond and the neighboring two π* orbitals of the phenyl moieties. It is clear that the enhanced electron withdrawing capability of o-carborane is a function of the geometrical preferences between the orbital overlap found in Ph2C2. As can be seen from the UV spectrum of **1**, further phenyl substitution at the boron atom relaxed the forbidden symmetrical excitations of the phenyl unit compared with that found in **3**. Thus, (1) "Ph2C2" unit is essential to lower the LUMO energy, which in turn manifests the electron withdrawing character of o-carborane, and (2) the phenyl unit orientation is important in maximizing this electron accepting property of o-carborane.

Cr coordination to the phenyl carbon atoms in **4** was confirmed by X-ray crystallography. Consistent with the geometrical change due to metal coordination, the absorption responsible for the LUMO energy is altered to

lower energy and the HOMO energy is altered to higher energy simultaneously, with a broad peak extending to 405 nm (see Figure S19 in Supplementary Information).
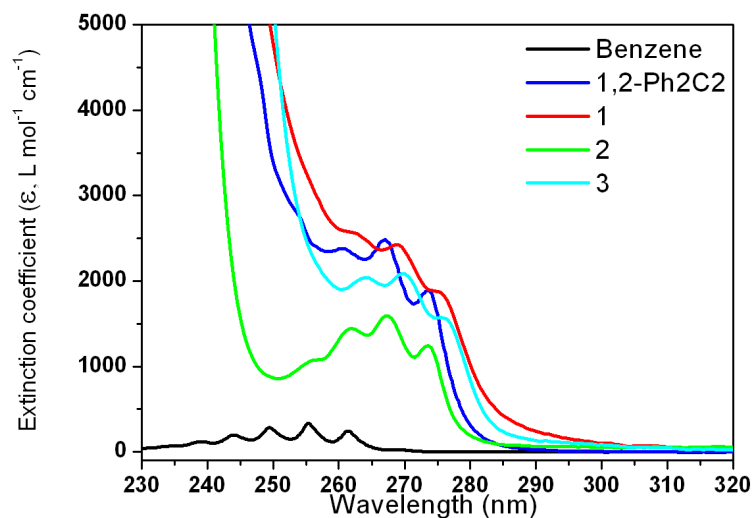

Figure 1. UV-vis absorption spectra of benzene, Ph2C2, **1**, **2**, and **3** in hexane solution at 25 °C.

As shown in Figure 2 and Figures S20–S25 (Supplementary Information), the Raman spectra of **1**–**4** differ markedly from those of the parent o-carborane; all exhibit low intensity and split peaks in the 725 ~ 780 cm^{-1} region. Among the carborane compounds, a low intensity and peak splitting pattern are more pronounced for the highly phenylated carboranes and their chromium complex, **1**–**4**. Figure 2 shows the Raman spectra of **1** in which the simulated DFT spectrum correlates well with the experimental spectrum. Compared with the Raman spectra of o-carborane and 1-phenyl-o-carborane (see Figures S20 and S21 in Supplementary Information), these data reveal that the 741, 777, and 789 cm^{-1} peaks are assignable to the vibrational modes around the o-carboranyl carbons of **1**. Moreover, the C=C stretching breathing mode occurs at 1002 cm^{-1} and the C=C–H quadrant stretching modes occur at 1236 cm^{-1} (D band) and 1602 cm^{-1} (G band) of phenyl rings [32].
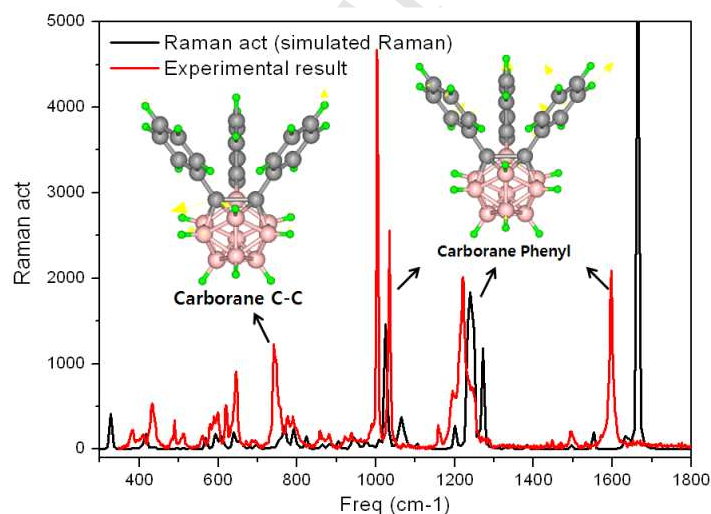

Figure 2. Simulated and experimental Raman spectra of **1** at 25 °C.

All other optical properties as well as electronic properties of CV data are presented in Table 1. A strong correlation exists between the orientation of the phenyl groups found in the X-ray structures and the electronic structure deduced from optical spectroscopy. The phenyl groups and their orientations correlate well to reversible reduction waves and their corresponding peak positions: **1** shows the lowest reduction potential among the series. Further, such differences also indicate the electronic alteration initiated by o-carborane and provide direct evidence of LUMO stabilization.

Table 1. Physical properties of Ph2C2 and 1-4.

Comp	λ_{abs} (nm)[a] [ε, M^{-1}, cm^{-1}]	E_{ox} (V)[b]	E_{red} (V)[b]
Ph2C2	224, 260, 267, 273 [33017, 2460, 2572, 1963]	–[c]	−2.05[d]
1	227, 261, 268, 277 [31887, 2627, 2479, 1954]	–[c]	−1.72[d]
2	223, 261, 267, 273 [33469, 1502, 1659, 1317]	–[c]	–[c]
3	230, 263, 269, 277 [42685, 2119, 2147, 1650]	–[c]	−2.25[d]
4	257, 327, 405 [11713, 7080, 1454]	0.49[e]	−1.41[d]

[a]Measured in Ar-saturated hexane solution (20 μM) at 25 °C. [b]Oxidation and reduction potentials measured for Ar-saturated dichloromethane solution by cyclic voltammetry (V vs Fc/Fc+). [c]Not detected. [d]Cathodic wave of one-electron reduction wave. [e]Anodic wave of one-electron oxidation wave.

As shown in Figure 3, the CV spectrum of **4** has one irreversible oxidation and one reversible reduction wave at 0.49 and −1.41 V, which correlate to the chromium (0/+1) metal center and the Ph2C2 unit, respectively. LUMO energy stabilization is clearly seen from Ph2C2, **1**, and **4**. Previously, a HOMO–LUMO gap of 5.78 eV for Ph2C2 was reported by measuring its UV-Vis spectrum. DFT/TDDFT calculations were performed on the tri- and tetra-phenyl-o-carboranes (**1**–**3**), and their geometries and geometrical parameters corresponded well to the X-ray crystallographic structures. As shown in the inset of Figure 3, the frontier orbitals of tri-phenyl-o-carborane **1** is largely centered on the B-substituted phenyl ring, with the HOMO-LUMO gap (5.23 eV) accounting, in part, for the stability of this compound. Moreover, the resulting simulated electronic spectra are in excellent agreement with those observed. Relative to **1**, the optimized geometry for chromium complex **4** reveals that the compositions of the LUMO frontier orbitals are similar to those found in the optimized geometry for **1**, and a small HOMO–LUMO gap (3.67 eV) was also observed in this compound. The LUMO is associated with the two C-substituted phenyl rings and partially carborane and chromium metal atoms.
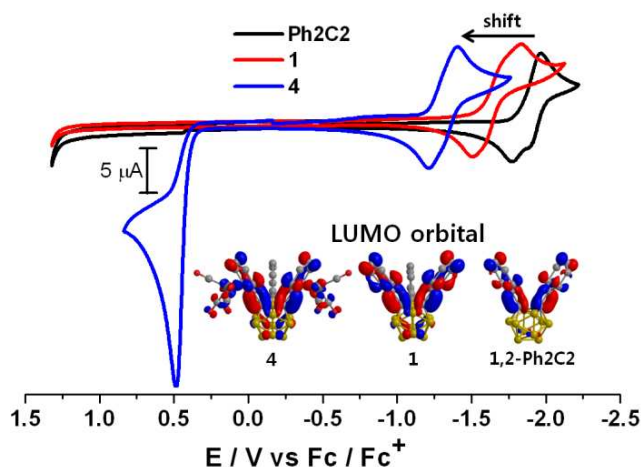
Figure 3. Cyclic voltammograms of Ph2C2, **1**, and **4** in CH_2Cl_2 solution (scan rate = 100 mV/s). (Inset: LUMO orbital analysis in the ground state.)

3.4 X-ray structural studies on tri-, tetra-phenyl-o-carboranes and its chromium complexes

Single crystal X-ray structure determination clearly revealed the structural authenticity of each compound and alluded to the electronic alteration from the investigation on the C−C distance: C−C bond distance is a direct measure of electronic alteration because it reflects the C−C σ* orbital's contribution and directly affected LUMO energy [33]. In this series, the C−C distance is the longest for **1** followed by **3** and is the shortest for **2**. Complexes **1** and **3** comprise further phenyl decorations at the boron atoms while maintaining the Ph2C2 platform active, whereas **2** contains one phenyl-free carbon atom [34].
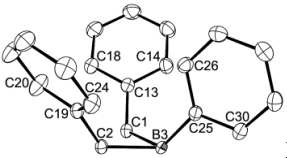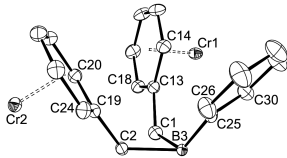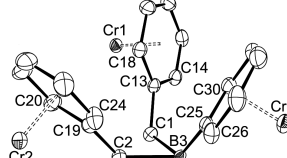
In line with the expectation of the C−C bond distance and LUMO energy stabilization, longer C−C bond distances correlate with a larger LUMO contribution, *vide infra*. It is now obvious that placement of two phenyl groups at the carbon atoms is the minimum requirement for LUMO stabilization. In addition, the conformation of the two phenyl groups at the carbon atoms can contribute greatly to the stabilization of LUMO. As can be seen in Figure 4, the structure of **1** has a special feature in which the additional phenyl unit, which is substituted at the boron atom, adopts a conformation to lock the two phenyl groups at the two carbon atoms into a rigid posture responsible for the LUMO stabilization. As shown in Figure 5, **2** does not possess a Ph2C2 platform, so LUMO stabilization is not seen. Finally, the phenylated carboranes of the neighboring boron atoms found in compound **3**, as shown in Figure 6, do not show sufficient LUMO stabilization, indicating that favorable phenyl π* and o-carboranyl C−C σ* orbital interactions do not occur in its conformation; indeed, in the solid structure of **3**, the two phenyl groups at the carbon atoms do not adopt the necessary face-to-face conformation for favorable interaction. The above can be summarized using the torsion angle between two phenyl planes with respect to the o-carboranyl C−C bond [35], in which perpendicular angles give rise to a face-to-face conformation and lead to a maximum C−C σ* orbital interaction, as found in **1**; a torsion angle of 88.73° for **1** can account for the superior orbital overlap. However, a smaller torsion angle for **3** (67.06°) appears to be due to steric interference by the B-phenyl groups. These results were communicated recently [36].

Single crystals of the B-phenylated triphenyl-o-carboranyl chromium complexes **4** and **5** suitable for X-ray

crystallography were obtained from toluene and dichloromethane solutions at slow evaporations. A comparison of the general structural features of **1** with its chromium complexes is given in Table 2. The corresponding molecular structures are illustrated in Figures 7 and 8. As shown in Figure 7, the chromium atoms in **4** are coordinated to phenyl rings in the cage carbon atoms in a π-bonding interaction. The chromium metals exhibit typical three-legged 'piano stool' geometries with expected geometrical parameters. The C−C bond lengths in the coordinated phenyl ring average 1.410 Å, which is 0.028 Å longer than the average bond length of 1.382 Å for C−C bonds within the non-coordinated phenyl ring. The Cr−C_{Ph} and Cr−CO bonds are in a normal range [37], having average values of 2.217 and 1.842 Å, respectively. The average C−O bond length in the chromium-coordinated carbonyl ligands is 1.147 Å, which is slightly shorter than that of $(\eta^6-C_6H_6)Cr(CO)_3$ [38]. Notably, this value is also slightly shorter than those of $[(\eta^6-C_6H_4-4-NH_2)(C_6H_5)]Cr(CO)_3$ [39] and $[(\eta^6-C_6H_5)(4-F-C_6H_4)]Cr(CO)_3$ [40]. As shown in Table 2, the chromium metals are centered approximately over the phenyl rings, giving rise to Cr1/Cr2−C_6H_5 face (centroid) distances of 1.701 and 1.710 Å, respectively. Furthermore, the C1−C2 bond length varies from **1** to **4**; it was shown that elongation of this bond is caused by favorable phenyl π* and o-carboranyl C−C σ* orbital interactions of the C1−C2 bond. As expected, the C1−C2 distance is the longest with a value of 1.776(3) Å, which lies essentially in the range of nonbonding character [41]. The C1−C13 bond is longer than that of **1** (C1-C13 1.518(**1**)/1.581(**4**) Å); however, the C2−C19 and B3−C25 bonds are shorter than that of **1** (C2−C19 1.513(**1**)/1.511(**4**), B3−C25 1.568(**1**)/1.510(**4**) Å). As shown in Table 2, the torsion angles of the three phenyl rings of **1** and **4** change with coordination of the chromium atoms.

The X-ray crystal structure of **5** (Figure 8) reveals that the tri-chromium atoms adopt an η^6-coordination with the three phenyl rings. Not surprisingly, the solid state structure of **5** shows many similarities to **4**. The geometrical parameters of this complex fall in the expected ranges (Table 2). The average C−C bond length in the chromium coordinated phenyl rings is 1.407 Å, which is identical to the value found for **1**, and which is 0.02 Å longer than the average bond length of 1.387 Å for C−C bonds within **1**. The Cr−C_{Ph} and Cr−CO bond lengths are in a normal range [36], having average values of 2.210 and 1.851 Å, respectively. The average C−O bond length in the chromium-coordinated carbonyl ligands is 1.139 Å, which is significantly shorter than those of $(\eta^6-C_6H_6)Cr(CO)_3$ [38], $[(\eta^6-C_6H_4-4-NH_2)(C_6H_5)]Cr(CO)_3$ [39] and $[(\eta^6-C_6H_5)(4-F-C_6H_4)]Cr(CO)_3$ [40]. As shown in Table 2, the chromium metals are centered approximately over the phenyl rings, giving rise to Cr1/Cr2/Cr3−C_6H_5 face (centroid) distances of 1.701, 1.705, and 1.708 Å, respectively. Interestingly, the C1−C2 bond length is shorter than that of **1**, it was shown that contraction of this bond is due to inadequate LUMO stabilization, indicating that favorable phenyl ring π* and carboranyl C−C σ* orbital interactions do not occur in **5**. The C1−C2 distance is the longest with the value of 1.748(4) Å, which lies essentially in the range of nonbonding character [41]. The C1−C13 and C2−C19 bond lengths are longer than those of **1** (C1−C13 1.518(**1**)/1.566(**4**), C2−C19 1.513(**1**)/1.529(**4**) Å), however, the B3−C25 bond is shorter than that of **1** (1.568(**1**)/1.506(**4**) Å). As shown in Table 2, the torsion angles of the three phenyl rings of **1** and **5** change with coordination of the chromium atoms.

Table 2. Comparison of bond lengths (Å) and torsion angles (°) for **1**, **4**, and **5**.

	1	4	5
Ph$_{C-C}$ (av)	1.3871	1.382	
Ph$_{C-C}$ (av)−Cr		1.410	1.407
Cab$_{C-C}$	1.764(2)	1.776(3)	1.748(4)
Cent−Cr		1.701, 1.710	1.701, 1.705, 1.708
C1-C2-C19-C20	62.3(2)	38.5(3)	65.3(3)
C1-B3-C25-C26	34.2(2)	130.4(2)	144.7(3)
B3-C1-C13-C18	−143.4(1)	170.5(2)	−64.1(4)
C2-C1-C13-C14	117.8(1)	60.9(3)	−173.4(2)
C2-B3-C25-C26	−39.2(2)	57.9(3)	75.5(3)
B3-C2-C19-C20	133.6(1)	107.7(2)	136.1(3)

In conclusion, we have found that the LUMO of Ph2C2 was stabilized through the B-phenylation found in **1**, and **1** functions as a strong π-acceptor to form a stable new type of organometallic complexes (**4** and **5**) through metal-to-ligand back-bonding interaction [Cr(d)−Ph(π*)−o-carboranyl C−C(σ*)]. This study clearly shows the electron withdrawing properties of o-carborane, provide that the two phenyl groups are positioned in a juxtaposed and paralleled fashion.

Acknowledgement

Appendix A. Supplementary material

CCDC 944100−944103 and 1813485 for compounds **1**, **2**, **3**, **4**, and **5** contains the supplementary crystallographic data for this paper. These data can be obtained free of charge from The Cambridge Crystallographic Data Centre via www.ccdc.cam.ac.uk/data_request/cif.

References

[1] (a) R. E. Williams, Chem. Rev. 92 (1992) 177. (b) M. F. Hawthorne, Advances in Boron Chemistry, Special Publication No. 201, Royal Society of Chemistry, London, 1997. (c) Y. Endo, T. Sawabe, Y. Taoda, J. Am. Chem. Soc. 122 (2000) 180. (d) F. Teixidor, R. Núñez, C. Viñas, R. Sillanpää, R. Kivekäs, Angew. Chem., Int. Ed. 39 (2000) 4290. (e) Z. Chen, R. B. King, Chem. Rev. 105 (2005) 3613. (f) R. Núñez, P. Farràs, F. Teixidor, C. Viñas, R. Sillanpää, R. Kivekäs, Angew. Chem., Int. Ed. 45 (2006) 1270.

[2] (a) M. A. Fox, J. A. K. Howard, J. A. H. MacBride, A. Mackinnon, K. Wade, J. Organomet. Chem. 680 (2003) 155. (b) J. J. Peterson, Y. C. Simon, E. B. Coughlin, K. R. Carter, Chem. Commun. (2009) 4950. (c) K. Kokado and Y. Chujo, Macromolecules 42 (2009) 1418. (d) B. P. Dash, R. Satapathy, E. R. Gaillard, J. A. Maguire, N. S. Hosmane, J. Am. Chem. Soc. 132 (2010) 6578. (e) B. P. Dash, R. Satapathy, E. R. Gaillard, K. M. Norton, J. A. Maguire, N. Chug, N. S. Hosmane, Inorg. Chem. 50 (2011) 5485. (f) N. S. Hosmane, Boron Science: New Technologies and Applications, CRC Press, New York, 2012.

[3] (a) J. Ko, S. O. Kang, Adv. Organomet. Chem. 47 (2001) 61. (b) Z. Xie, Acc. Chem. Res. 36 (2003) 1. (c) N. S. Hosmane, J. A. Maguire, Organometallics 24 (2005) 1356. (d) R. Satapathy, B. P. Dash, J. A. Maguire, N. S. Hosmane, Dalton Trans. 39 (2010) 6613. (e) P. Dröse, C. G. Hrib, T. F. Edelmann, J. Am. Chem. Soc. 132 (2010) 15540. (f) Z. Qiu, S. Ren, Z. Xie, Acc. Chem. Res. 44 (2011) 299. (g) Z. -J. Yao, X. -K. Huo, G. -X. Jin, Chem. Commun. 48 (2012) 6714.

[4] (a) M. A. Fox, C. Nervi, A. Crivello, A. S. Batsanov, J. A. K. Howard, K. Wade, P. J. Low, J. Solid State Electrochem. 13 (2009) 1483. (b) H. Tricas, M. Colon, D. Ellis, S. A. Macgregor, D. McKay, G. M. Rosair, A. J. Welch, I. V. Glukhov, F. Rossi, F. Laschi, P. Zanello, Dalton Trans. 40 (2011) 4200.

[5] K. -R. Wee, W. -S. Han, D. W. Cho, S. Kwon, C. Pac, S. O. Kang, Angew. Chem., Int. Ed. 51 (2012) 2677.

[6] R. N. Grimes, Carboranes, 2nd ed., Academic Press (Elsevier), New York, 2011.

[7] a) J. Llop, C. Viñas, J. M. Oliva, F. Teixidor, M. A. Flores, R. Kivekäs, R. Sillanpää, J. Organomet. Chem. 657 (2002) 232. b) L. A. Boyd, W. Clegg, R. C. B. Copley, M. G. Davidson, M. A. Fox, T. G. Hibbert, J. A. K. Howard, A. Mackinnon, R. J. Peace, K. Wade, Dalton Trans. (2004) 2786. c) J. M. Oliva, N. L. Allan, P. v. R. Schleyer, C. Viñas, F. Teixidor, J. Am. Chem. Soc. 127 (2005) 13538.

[8] A. R. Turner, H. E. Robertson, K. B. Borisenko, D. W. H. Rankin, M. A. Fox, Dalton Trans. (2005) 1310.

[9] B.W. Hutton, F. MacIntosh, D. Ellis, F. Herisse, S. A. Macgregor, D. McKay, V. Petrie-Armstrong, G. M. Rosair, D. S. Perekalin, H. Tricas, A. J. Welch, Chem. Commun. (2008) 5345.

[10]. K. Chui, H.-W. Li, Z. Xie, Organometallics 19 (2000) 5447.

[11] a) K. Kokado, A. Nagai, Y. Chujo, Tetrahedron Lett. 52 (2011) 293. b) K. Kokado, Y. Chujo, Dalton Trans. 40 (2011) 1919. c) K. Kokado, Y. Chujo, J. Org. Chem. 76 (2011) 316. d) J. J. Peterson, A. R. Davis, M. Werre, E. B. Coughlin, K. R. Carter, ACS Appl. Mater. Interfaces 3 (2011) 1796. e) A. R. Davis, J. J. Peterson, K. R. Carter, ACS Macro Lett. 1 (2012) 469. f) K. -R. Wee, Y. -J. Cho, S. Jeong, S. Kwon, J. -D. Lee, I. -H. Suh, S. O. Kang, J. Am. Chem. Soc. 134 (2012) 17982. g) S. Inagi, K. Hosoi, T. Kubo, N. Shida, T. Fuchigami,

Electrochemistry 81 (2013) 368. h) H. J. Bae, H. Kim, K. M. Lee, T. Kim, Y. S. Lee, Y. Do, M. H. Lee, Dalton Trans. 43 (2014) 4978.

[12] L. Weber, J. Kahlert, R. Brockhinke, L. Bchling, A. Brockhinke, H. -G. Stammler, B. Neumann, R. A. Harder, M. A. Fox, Chem. Eur. J. 18 (2012) 8347.

[13] L. Weber, J. Kahlert, L. Bchling, A. Brockhinke, H. -G. Stammler, B. Neumann, R. A. Harder, P. J. Low, M. A. Fox, Dalton Trans. 42 (2013) 2266.

[14] A. J. Welch, *Steric Effects in Metallacarboranes*, in *Metal Clusters in Chemistry* (Eds.: P. Braunstein, L. A. Oro and P. R. Raithby), Wiley-VCH, 1999, 69.

[15]. (a) M. F. Semmelhack, in: E. W. Abel, F. G. A. Stone, G. Wilkinson (Eds.), Comprehensive Organometallic Chemistry II, vol. 12, Pergamon Press, Oxford, 1995, p. 979; (b) F. Rose-Munch, E. Rose, Current Org. Chem. 3 (1999) 445. (c) F. Rose-Munch, E. Rose, in: D. Astruc (Ed.), Modern Arene Chemistry, Wiley-VCH, 2002, pp. 368−397 (Chapter 11).

[16]. T. R. Jonson, B. E. Mann, J. E. Clark, R. Foresti, C. J. Green, R. Motterlini, Angew. Chem., Int. Ed. 42 (2003) 3722.

[17] (a) G. Jaouen, A. Vessières, I. Butler, Acc. Chem. Res. 26 (1993) 361. (b) A. Hess, N. Metzler-Nolte, Chem. Commun. (1999) 885. (c) C. Baldoli, S. Maiorana, E. Licandro, G. Zinzalla, D. Perdicchia, Org. Lett. 4 (2002) 4341.

[18] *SMART and SAINT*; Bruker Analytical X-Ray Division: Madison, WI, 2002.

[19] G. M. Sheldrick, *SHELXTL-PLUS Software Package*; Bruker Analytical X-Ray Division: Madison, WI, 2002.

[20] (a) C. Lee, W. Yang, R. G. Parr, R. Phys. Rev. B 37 (1988) 785. (b) S. H. Vosko, L. Wilk, M. Nusair, Can. J. Phys. 58 (1980) 1200. (c) A. D. Becke, J. Chem. Phys. **98 (**1993) 5648. (d) P. J. Stephens, F. J. Devlin, C. F. Chabalowski, M. J. Frisch, J. Phys. Chem. 98 (1994) 11623.

[21] P. J. Hay, W. R. Wadt, J. Chem. Phys. 82 (1985) 299.

[22] (a) "Gaussian Basis Sets for Molecular Calculations" S.Huzinaga, J.Andzelm, M.Klobukowski, E.Radzio-Andzelm, Y.Sakai, H.Tatewaki Elsevier, Amsterdam, 1984. (b) E. R. Davidson, D. Feller, Chem. Rev. 86 (1986) 681.

[23] M. J. Frisch, G. W. Trucks, H. B. Schlegel, G. E. Scuseria, M. A. Robb, J. R. Cheeseman, G. Scalmani, V. Barone, B. Mennucci, G. A. Petersson, H. Nakatsuji, M. Caricato, X. Li, H. P. Hratchian, A. F. Izmaylov, J. Bloino, G. Zheng, J. L. Sonnenberg, M. Hada, M. Ehara, K. Toyota, R. Fukuda, J. Hasegawa, M. Ishida, T. Nakajima, Y. Honda, O. Kitao, H. Nakai, T. Vreven, J. A. Montgomery Jr., J. E. Peralta, F. Ogliaro, M. Bearpark, J. J. Heyd, E. Brothers, K. N. Kudin, V. N. Staroverov, T. Keith, R. Kobayashi, J. Normand, K. Raghavachari, A.

Rendell, J. C. Burant, S. S. Iyengar, J. Tomasi, M. Cossi, N. Rega, J. M. Millam, M. Klene, J. E. Knox, J. B. Cross, V. Bakken, C. Adamo, J. Jaramillo, R. Gomperts, R. E. Stratmann, O. Yazyev, A. J. Austin, R. Cammi, C. Pomelli, J. W. Ochterski, R. L. Martin, K. Morokuma, V. G. Zakrzewski, G. A. Voth, P. Salvador, J. J. Dannenberg, S. Dapprich, A. D. Daniels, O. Farkas, J. B. Foresman, J. V. Ortiz, J. Cioslowski, D. J. Fox, Gaussian 09, Revision B.01, Gaussian, Inc., Wallingford CT, 2010.

[24] Chem3D Ultra 9.0 for PC, CambridgeSoft, 100 CambridgePark Drive, Cambridge, MA 02140.

[25] N. M. O'Boyle, A. L. Tenderholt, K. M. Langner, K. M. J. Comput. Chem. 29 (2008) 839.

[26] (a) T. L. Heying, J. W. Ager, Jr., S. L. Clark, D. J. Mangold, H. L. Goldstein, M. Hillman, R. J. Polak, J. W. Szymanski, Inorg. Chem. 2 (1963) 1089. (b) R. Coult, M. A. Fox, W. R. Gill, P. L. Herbertson, J. A. H. MacBride, K. Wade, J. Organomet. Chem. 462 (1993) 19. (c) K. Ohta, T. Goto, Y. Endo, Inorg. Chem. 44 (2005) 8569. (d) K. Aizawa, K. Ohta, Y. Endo, Heterocycles, 80 (2010) 3697.

[27] M. F. Hawthorne, P. A. Wegner, J. Am. Chem. Soc. 90 (1968) 896.

[28] (a) A. V. Safronov, Y. V. Sevryugina, S. S. Jalisatgi, R. D. Kennedy, C. L. Barnes, M. F. Hawthorne, Inorg. Chem. 51 (2012) 2629. (b) J. Holub, M. Bakardjiev, B. Štíbr, P. Štěpnička and I. Císařová, Eur. J. Inorg. Chem. (2010) 4196.

[29]. T. J. Henly, C. B. Knobler, M. F. Hawthorne, Organometallics 11 (1992) 2313.

[30] (a) C. A. L. Mahaffy, P. L. Pauson, Inorg. Synth. 19 (1979) 154. (b) R. D. Fischer, Chem. Ber. 93 (1960)165. (c) D. A. Brown, H. Sloan, J. Chem. Soc. (1963) 4389. (d) D. A. Brown, J. R. Raju, J. Chem. Soc. A. (1966) 1617. (e) D. M. Adams, A. Squire, J. Chem. Soc., Dalton Trans. (1974) 558.

[31] I. B. Berlman, Handbook of Fluorescence Spectra of Aromatic Molecules, Academic Press, N.Y, 1971.

[32] (a) A. Criado, M. Melchionna, S. Marchesan, M. Prato, Angew. Chem. Int. Ed. 54 (2015) 10734. (b) V. Barone, M. Biczysko, J. Bloino, Phys. Chem. Chem. Phys. 16 (2014) 1759. (c) D. B. Menezes, A. Reyer, A. Marletta, M. Musso, Mater. Res. Express 4 (2017) 015303.

[33] M. A. Fox, C. Nervi, A. Crivello, P. J. Low, Chem. Commun. (2007) 2372.

[34] (a) L. A. Boyd, W. Clegg, R. C. B. Copley, M. G. Davidson, M. A. Fox, T. G. Hibbert, J. A. K. Howard, A. Mackinnon, R. J. Peace, K. Wade, Dalton Trans. (2004) 2786. (b) M. A. Fox, R. J. Peace, W. Clegg, M. R. J. Elsegood, K. Wade, Polyhedron 28 (2009) 2359.

[35] (a) E. S. Alekseyeva, M. A. Fox, J. A. K. Howard, J. A. H. MacBride, K. Wade, Appl. Organomet. Chem. 17 (2003) 499. (b) L. Weber, J. Kahlert, R. Brockhinke, L. Bchling, A. Brockhinke, H. -G. Stammler, B. Neumann, R. A. Harder, M. A. Fox, Chem. Eur. J. 18 (2012) 8347.

[36] G. F. Jin, J. –H. Hwang, J. –D. Lee, K. –R. Wee, I. –H. Suh, S. O. Kang, Chem. Comm. 49 (2013) 9398.

[37] M. J. Calhorda, C. F. Frazão, J. A. Martinho-Simões, J. Organomet. Chem. 262 (1984) 305.

[38] (a) B. Rees, P. Coppens, Acta Crystallogr., Sect. B 29 (1973) 2515. (b) M. F. Bailey, L. F. Dahl, Inorg. Chem. 4 (1965) 1314. (c) G. Allegra, G. Natta, Atti Accad. Naz. Lincei 31 (1961) 241. (d) Y. Wang, K. Angermund, R. Goddard, C. Kruger, J. Am. Chem. Soc. 109 (1987) 587.

[39] C. J. Czerwinski, I. A. Guzei, K. M. Riggle, J. R. Schroeder, L. C. Spencer, Dalton Trnas. 40 (2011) 9439.

[40] I. A. Guzei, L. C. Spencer, S. C. Buechel, L. B. Kaufmann, C. J. Czerwinski, Acta Cryst. C73 (2017) 638.

[41] (a) M. G. Davidson, T. G. Hibbert, J. A. K. Howard, A. Mackinnon, K. Wade, Chem. Commun. (1996) 2285. (b) J. Llop, C. Viñas, J. M. Oliva, F. Teixidor, M. A. Flores, R. Kivekäs, R. Sillanpää, J. Organomet. Chem. 657 (2002) 232; (c) J. M. Oliva, N. L. Allan, P. v. R. Schleyer, C. Viñas and F. Teixidor, J. Am. Chem. Soc. 127 (2005) 13538. (d) B. W. Hutton, F. MacIntosh, D. Ellis, F. Herisse, S. A. Macgregor, D. McKay, V. P. Armstrong, G. M. Rosair, D. S. Perekalin, H. Tricas, A. J. Welch, Chem. Commun. (2008), 5345.
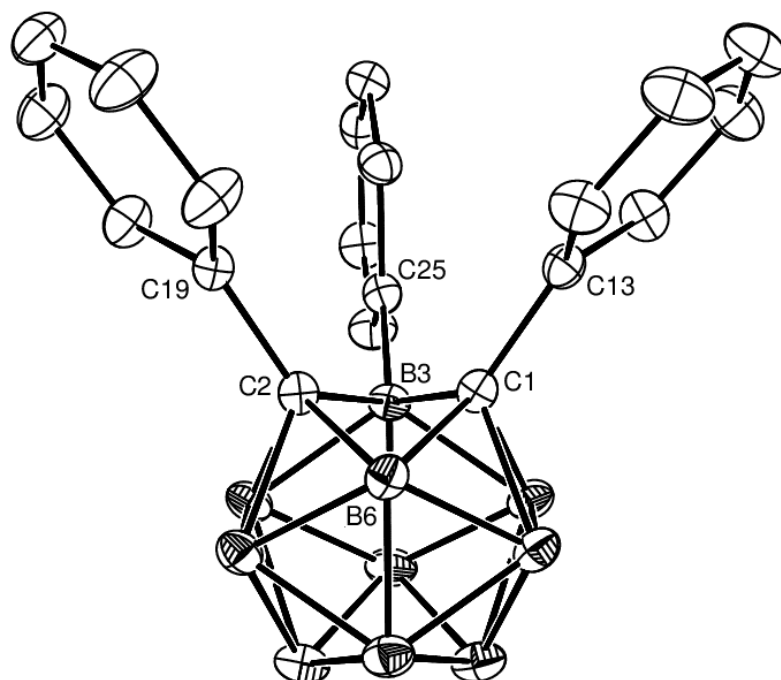
Figure 4. ORTEP drawing (30% probability for thermal ellipsoids) of **1** (the hydrogen atoms are omitted for clarity).
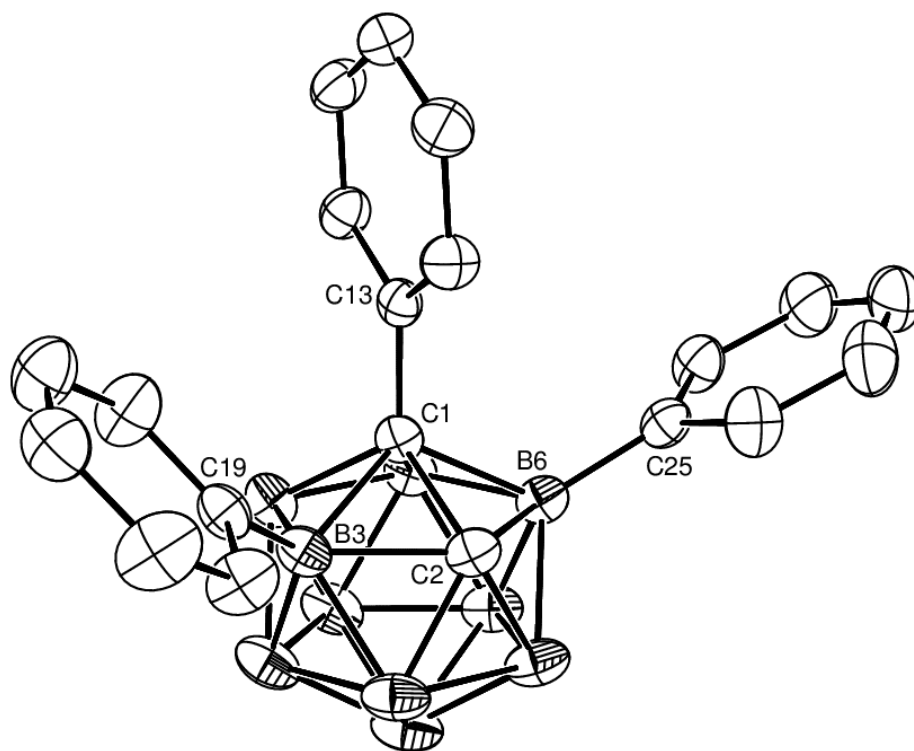
Figure 5. ORTEP drawing (30% probability for thermal ellipsoids) of **2** (the hydrogen atoms are omitted for clarity).
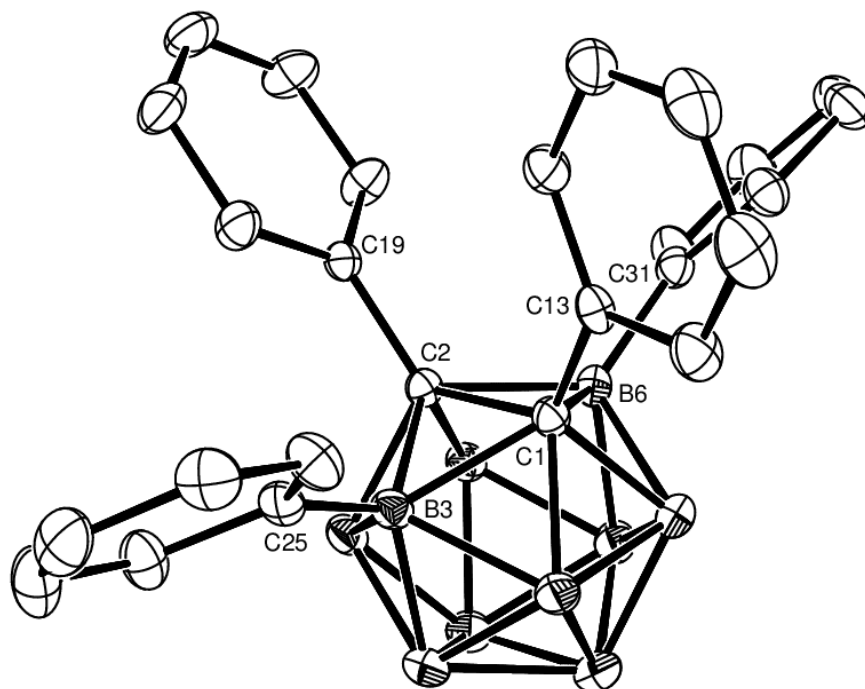
Figure 6. ORTEP drawing (30% probability for thermal ellipsoids) of **3** (the hydrogen atoms are omitted for clarity).
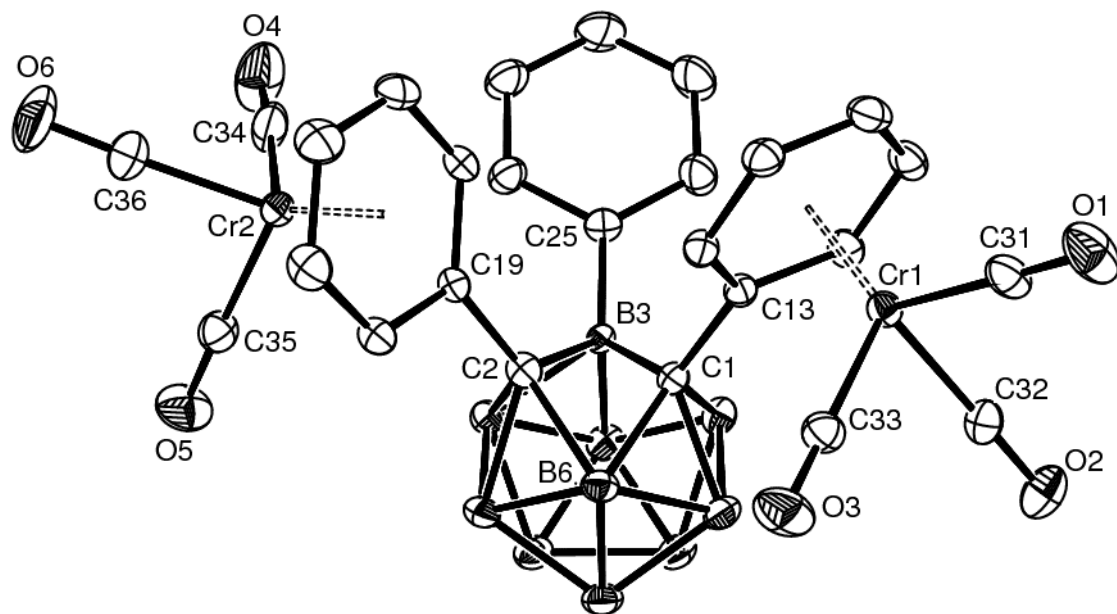
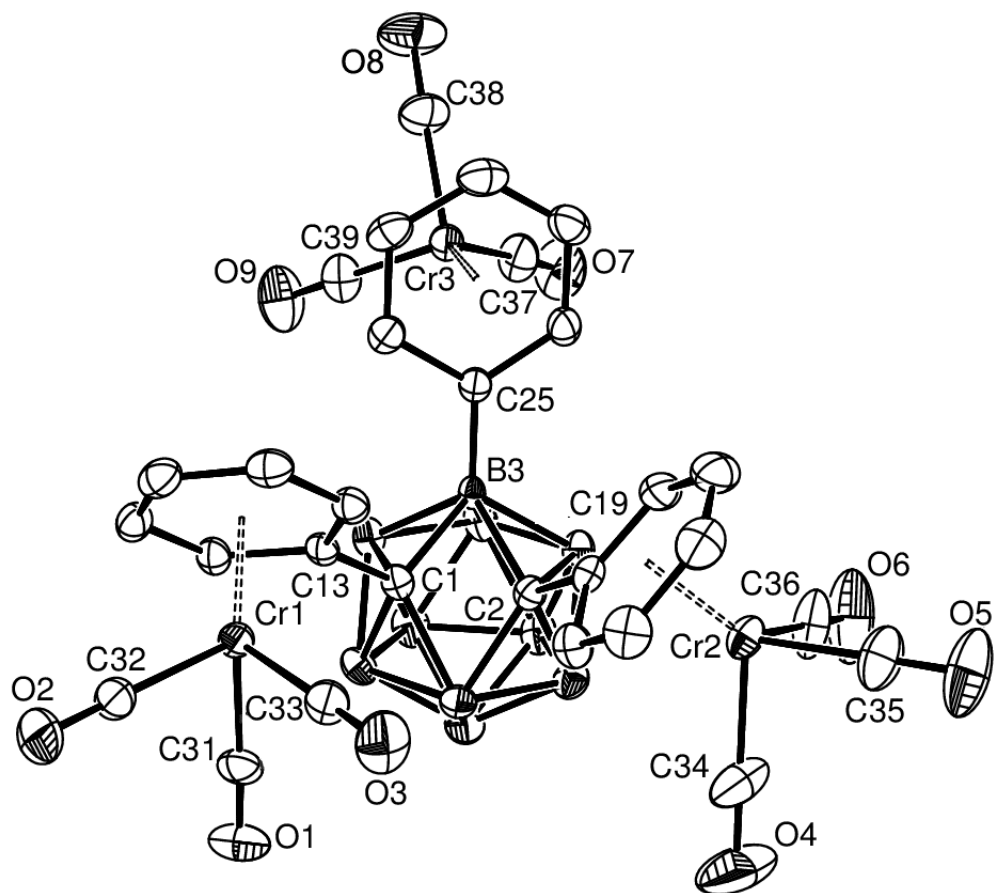**Figure 7**. ORTEP drawing (30% probability for thermal ellipsoids) of **4** (the hydrogen atoms are omitted for clarity).

Figure 8. ORTEP drawing (30% probability for thermal ellipsoids) of **5** (the hydrogen atoms are omitted for clarity).

Table 3. Crystal data and structure refinement of **1**, **2**, **3**, **4**, and **5**.

	1	2	3	4	5
Identification code	k110211	k111101	k120303	k120304	k140710
Empirical formula	$C_{20} H_{24} B_{10}$	$C_{20} H_{24} B_{10}$	$C_{26} H_{28} B_{10}$	$C_{26} H_{24} B_{10} Cr_2 O_6$	$C_{29} H_{24} B_{10} Cr_3 O_9 \cdot C H_2 Cl_2$
Formula weight	372.49	372.49	448.58	644.55	865.51
Temperature	293(2) K	293(2) K	293(2) K	293(2) K	293(2) K
Wavelength	0.71073 A	0.71073 Å	0.71073 Å	0.71073 A	0.71073 A
Crystal system, space group	Monoclinic,	Monoclinic,	Monoclinic,	Monoclinic,	Orthorhombic,
Unit cell dimensions	$P2_12_12_1$	$P2_1/n$	$P2_1/c$	$P 2_1/c$	$P 2_12_12_1$
	$a = 8.2745(7)$ Å	$a = 12.5359(8)$ Å	$a = 18.545(3)$ Å	$a = 16.531(3)$ Å	$a = 12.783(2)$ Å
	$b = 15.5626(13)$ Å	$b = 12.9150(8)$ Å	$b = 10.3481(15)$ Å	$b = 11.276(2)$ Å	$b = 14.909(2)$ Å
	$c = 16.2094(14)$ Å	$c = 13.3882(8)$ Å	$c = 13.6761(19)$ Å	$c = 15.770(3)$ Å	$c = 19.618(2)$ Å
Volume	2087.3(3) Å^3	2137.1(2) Å^3	2484.3(6) Å^3	2929.1(9) Å^3	3738.7(8) Å^3
Z, D_{calc}	4, 1.185 g/cm^3	4, 1.158 g/cm^3	4, 1.199 g/cm^3	4, 1.462 g/cm^3	4, 1.538 g/cm^3
$F(000)$	776	776	936	1304	1736
Crystal size	$0.10 \times 0.08 \times 0.05$ mm	$0.40 \times 0.20 \times 0.20$ mm	$0.2 \times 0.15 \times 0.1$ mm	$0.3 \times 0.2 \times 0.15$ mm	$0.2 \times 0.2 \times 0.15$ mm
θ range for data collection	1.81 to 28.34º	2.06 to 28.36º	1.16 to 28.43º	1.24 to 28.31º	1.72 to 28.29º
Limiting indices	$-11 \leq h \leq 10, -20 \leq k \leq 20, -21 \leq l \leq 21$	$-16 \leq h \leq 16, -17 \leq k \leq 17, -17 \leq l \leq 17$	$-24 \leq h \leq 24, -13 \leq k \leq 13, -18 \leq l \leq 18$	$-22 \leq h \leq 22, -15 \leq k \leq 14, -20 \leq l \leq 21$	$-17 \leq h \leq 17, -19 \leq k \leq 19, -26 \leq l \leq 26$

Reflections collected / unique	21438 / 5180 [R(int) = 0.0326]	28537 / 5335 [R(int) = 0.0335]	24319 / 6192 [R(int) = 0.0750]	29354 / 7259 [R(int) = 0.0281]	51105 / 9261 [R(int) = 0.0287]
Completeness to θ = 25.96	99.9 %	99.8 %	99.0 %	99.6 %	99.9 %
Refinement method	Full-matrix least-squares on F^2	Full-matrix least-squares on F^2	Full-matrix least-squares on F^2	Full-matrix least-squares on F^2	Full-matrix least-squares on F^2
Data / restraints / parameters	5180 / 0 / 271	5335 / 0 / 280	6192 / 0 / 333	7259 / 0 / 406	9261 / 0 / 496
Goodness-of-fit on F^2	1.019	1.054	1.055	1.060	1.027
Final R indices [I>2θ (I)]	[a]R_1 = 0.0427, [b]wR_2 = 0.1155	[a]R_1 = 0.0592, [b]wR_2 = 0.1565	[a]R_1 = 0.0758, [b]wR_2 = 0.1846	R_1 = 0.0422, wR_2 = 0.1228	R_1 = 0.0426, wR_2 = 0.1195
R indices (all data)	[a]R_1 = 0.0458, [b]wR_2 = 0.1190	[a]R_1 = 0.0770, [b]wR_2 = 0.1759	[a]R_1 = 0.1346, [b]wR_2 = 0.2137	R_1 = 0.0558, wR_2 = 0.1359	R_1 = 0.0479, wR_2 = 0.1255
Largest diff. peak and hole	0.263 and –0.191 e.Å^{-3}	0.270 and –0.305 e.Å^{-3}	0.292 and –0.269 e.Å^{-3}	0.782 and –0.574 e.Å^{-3}	0.728 and –0.485 e.Å^{-3}

[a]$R_1 = \sum||F_o|-|F_c||$ (based on reflections with $F_o^2 > 2\sigma F^2$), [b]$wR_2 = [\sum[w(F_o^2-F_c^2)^2]/\sum[w(F_o^2)^2]]^{1/2}$; $w = 1/[\sigma^2(F_o^2)+(0.095P)^2]$; , $P = [\max(F_o^2, 0)+2F_c^2]/3$ (also with $F_o^2 > 2\sigma F^2$)

Research Highlights

- ➢ Synthesis of 1,2,3- and 1,3,6-triphenyl-o-carboranes and 1,2,3,6-tetraphenyl-o-carborane using 1-phenyl-o-carborane and 1,2-diphenyl-o-carborane.
- ➢ Synthesis of $(1,2,3\text{-Ph}_3\text{-}1,2\text{-C}_2\text{B}_{10}\text{H}_9)[\text{Cr(CO}_3)]_2$ and $(1,2,3\text{-Ph}_3\text{-}1,2\text{-C}_2\text{B}_{10}\text{H}_9)[\text{Cr(CO)}_3]_3$ by 1,2,3-triphenyl-o-carborane with Cr(CO)6.
- ➢ The structures of the B-phenylated o-carboranes and its chromium complexes were studies by X-ray crystallography.
- ➢ We have found that the LUMO energy of Ph2C2 was stabilized through the B-phenylation found in Ph3C2B.